THE ASTROPHYSICAL JOURNAL, 297:751–765, 1985 October 15

A WIDE-LATITUDE CO SURVEY OF MOLECULAR CLOUDS IN THE NORTHERN MILKY WAY

T. M. DAME AND P. THADDEUS
Goddard Institute for Space Studies, and Departments of Physics and Astronomy, Columbia University
Received 1985 March 4; accepted 1985 April 22

ABSTRACT

Molecular clouds in the galactic quadrant from $l = 12°$–$100°$ were surveyed in the 115.271 GHz line of CO at an angular resolution of 1°. In galactic latitude the survey extends from $b = -5°$ to $+6°$, with extensions to higher latitude between $l = 20°$ and 60°. CO line emission, detected from 50% of the region surveyed, comes nearly equally from local clouds associated with the Great Rift in the Milky Way and from distant clouds in the inner arms of the Galaxy 4–7 kpc from the galactic center. Using the CO radial velocities, it was possible to resolve the Rift into 10 molecular clouds 200–2300 pc away, to associate many of these with optical objects (dark nebulae, OB associations, etc.), and to determine distances and masses. The nearby clouds of the Rift system have masses between a few times 10^4 and a few times 10^5 $M_\odot$, not large with respect to the largest clouds or cloud complexes found elsewhere in the galaxy; they are conspicuous mainly because they are close. The mean half-thickness at half-intensity of local molecular gas is estimated to be 75 ± 25 pc, in agreement with that obtained at the solar circle by other CO surveys, and the mean molecular density at midplane is 0.013 $M_\odot$ pc^{-3}. The correlation between the integrated CO line intensity and optical obscuration throughout the region of the survey is close, demonstrating that nearly all dark nebulae are molecular clouds, and vice versa.

Subject headings: galaxies: Milky Way — galaxies: structure — interstellar: molecules

I. INTRODUCTION

To investigate molecular clouds associated with the Great Rift in the Milky Way and the diffuse component of galactic gamma rays, we undertook a wide-latitude, low angular resolution survey of CO along most of the first galactic quadrant and part of the second. The survey, summarized in Table 1, is uniform and well sampled in galactic longitude from 12° to 100° and in latitude from −5° to +6°, with extensions as high as +11° to include specific dark clouds; the total area surveyed, 1400 deg^2, is a much larger region than has previously been studied in CO or other interstellar molecules. Both because of the great extent of the Rift and the low angular resolution of the *COS B* and *SAS 2* gamma-ray surveys ($\gtrsim 2°$), angular resolution was sacrificed for coverage and speed, a resolution of 1° being chosen to allow the survey to be completed in two observing seasons on the Goddard-Columbia 1.2 m telescope.

A brief description of the telescope and of the way the survey data were obtained is given in the next section. Section III presents the basic survey results and compares them with results of the deep Columbia survey of the inner galaxy done with the same instrument at full angular resolution. The discussion in § IV is devoted to the gamma-ray comparison and to the H_2/CO ratio derived from it. The masses and other properties of the main molecular clouds identified in the survey are discussed in § V, and in § VI these clouds are used to investigate the scale height and average density of local molecular gas.

TABLE 1

PARAMETERS OF THE SURVEY

Galactic longitude	12°–100°
Galactic latitude	$l < 60°$: −4°–+9° $l > 60°$: −4°–+6°
Radial velocity	$l < 60°$, $\lvert b\rvert < 3°$: −13–153 km s^{-1} $l > 60°$, $\lvert b\rvert < 3°$: −113–53 km s^{-1} all l, $\lvert b\rvert \geq 3°$: −83–83 km s^{-1}
Angular resolution	1°
Sampling interval	1°
Velocity resolution	0.65 km s^{-1}
Sensitivity	$T_R = 0.3$ K rms at $\Delta v = 1.3$ km s^{-1}

II. INSTRUMENTATION AND DATA TAKING

The antenna of the 1.2 m telescope is a fast Cassegrain with an f/D ratio of 0.375 at the primary focus and 2.8 at the feed horn at the secondary focus. Its full beamwidth at half-intensity with the scalar feed used for the work here, measured with a 115 GHz transmitter on a distant building, was $8\farcm7 \pm 0\farcm1$, in agreement with that calculated from scalar diffraction theory. Pointing was demonstrated to be better than 1′ by observing a number of bright stars with a small optical telescope previously coaligned with the radio beam to better than 30″ by centering both on the solar disk. A list of the important telescope parameters is given in Table 2.

An angular resolution of 1° was produced by simply scanning a square 8 × 8 raster of points separated by $\frac{1}{8}$° and summing the resultant 64 spectra at the end of an observation. Although it offers no theoretical gain in the rate at which information is acquired, this procedure is preferable for practical reasons to underilluminating or stopping-down the tele-

TABLE 2

PARAMETERS OF TELESCOPE AT 115 GHz DURING SURVEY

Beamwidth (FWHM)	$8\farcm7 \pm 0\farcm1$
Beam efficiency	0.79
Pointing	<1 rms
Receiver noise temperature	450 K (double sideband)
Spectrometer	256 filters, each 250 kHz wide

scope to achieve a 1° beam. Implemented entirely by computer software, the procedure allows the telescope immediately to revert for other work to full resolution without any modification of the antenna or change of the feed and allows reference OFF positions the size of the $\frac{1}{8}$° primary beam of the telescope, which, then, enabled us to adopt the OFFs used in our deep survey of the galactic plane (Cohen, Dame, and Thaddeus 1985), at a considerable saving of time. Owing to the greater extent of the present survey, these OFFs were necessarily supplemented by additional OFFs (Fig. 3*c*) which, selected like the old to lie in obscuration-free regions on the Palomar Sky Survey prints, were then shown by frequency switching or by position switching against one another, or both, to be free of CO line emission to a level of ~0.2 K.

Both in elevation and azimuth the 1.2 m telescope is driven without a gear train by direct-drive torque motors and can position-switch rapidly over angles as large as 10°. The spectra of the present survey were obtained by switching with a full period of 30 s until the rms noise in the "final" spectrum (i.e., the sum of the 64 spectra in a given 1° raster) fell below a specified level: 0.3 K when the spectrum was smoothed over two channels to a velocity resolution of 1.3 km s^{-1}. Slight baseline curvature, sometimes encountered when ON and OFF positions were separated by more than a few degrees, was eliminated by surrounding the point under observation with three OFFs, the time on each adjusted automatically by the telescope's guidance computer so that the time-weighted average of the displacement vectors to the OFFs was zero. Figure 1 shows a sample of the spectra obtained in the survey that illustrates the excellent flatness of the baselines.

The total observation time, including OFF positions, needed to achieve the desired noise level under good atmospheric conditions was typically 15 minutes. Altogether, the survey represents ~500 hr of observation. Most spectra were obtained on cold, dry days in 1979 and 1980, the observing season of the telescope generally extending from October to May.

The superheterodyne receiver used consisted of an uncooled Schottky barrier mixer followed by an uncooled 1420 MHz parametric amplifier with a noise temperature of 50 K, a combination which yielded a double sideband noise temperature of ~450 K. No attempt was made to filter out the image sideband, that was placed below the CO line at 112.4 GHz where, owing to the greater distance to the telluric O_2 transition at 118.7 GHz, the atmosphere is somewhat more transparent. No significant interstellar lines fall in the image sideband. The spectrometer was a filter bank of 256 channels, each 250 kHz wide, that yielded a resolution in radial velocity of 0.65 km s^{-1} and a spectral range of 166 km s^{-1}.

The intensity of the spectra were calibrated conventionally and corrected for atmospheric absorption by rotating a small room-temperature blackbody chopper wheel in front of the feed for a few seconds before each integration (Penzias and Burrus 1973; Kutner 1978). The temperature and opacity of atmospheric water vapor required by this method of calibration were measured by antenna tipping every 6 hr when atmospheric conditions were steady and more often when variable.

The calibration and the efficiency of the 1.2 m telescope have been closely checked against two larger instruments widely used for CO observations: the NRAO 11 m telescope and the Bell 7 m telescope. The comparison was done by smoothing a well-sampled CO map of a standard source from each larger telescope to a resolution of 8′. The radiation temperature (i.e., antenna temperature corrected for atmospheric absorption and beam efficiency) measured with the 1.2 m telescope toward Orion A was 8% greater than that obtained from the convolved NRAO map, while the temperature toward the center of B335 was 17% less than that obtained from the convolved Bell map. Since the calibration of large telescopes is generally reproducible to only 10%–20% on changing receivers, feeds, and antenna surfaces, which means it is uncertain to roughly this figure, we conclude that our calibration agrees satisfactorily with these larger instruments. Finally, a continuum measurement of the Sun at 115 GHz with the 1.2 m telescope agrees with that measured with standard horns (Linsky 1973) after correcting for an estimated forward coupling efficiency.

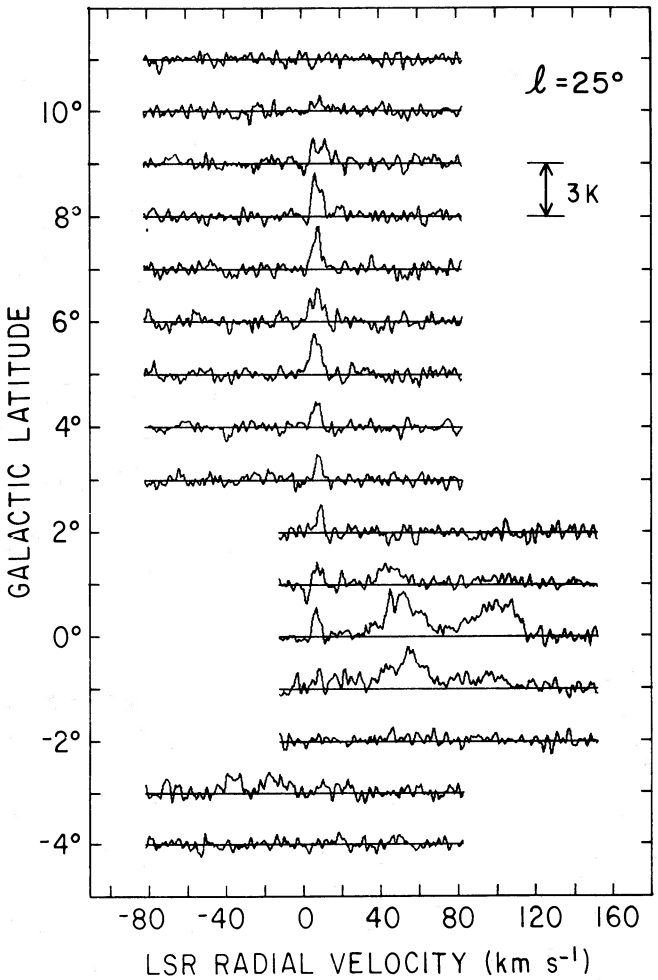

FIG. 1.—Sample CO spectra: the survey at $l = 25°$. Note the very flat baselines far from the galactic plane where CO emission is absent, e.g., at $b = +11°$, $+10°$, $-4°$. Spectra were smoothed slightly to a velocity resolution of 1.3 km s^{-1} from the filter width of 0.65 km s^{-1}, and a small constant offset and slope were removed; otherwise they are unprocessed. At latitudes 3° from the plane and more the spectrometer was centered on 0 km s^{-1}; closer it was centered as shown at +70 km s^{-1} to capture distant molecular clouds in the inner galaxy.

III. SURVEY RESULTS

To summarize the survey concisely in two-dimensional maps, the CO spectra were numerically integrated over radial velocity to display the molecular clouds on the plane of the sky, with no indication of velocity or kinematic distance relative to the observer, and over galactic latitude to obtain stan-

dard longitude-velocity diagrams that display velocity without indicating how far off the galactic plane the clouds lie.

Figure 3*a*, the plane-of-the-sky map obtained when the velocity integration covers the full range of the spectrometer, includes all material within the solar circle in the longitude range of the survey, as Figure 2 shows, and some beyond. At longitudes below 60° some unresolved distant clouds have undoubtedly been missed, but the decrease in the number of molecular clouds is so rapid beyond the solar circle that this limitation of the survey is minor; were the spectral range of the receiver wide enough to cover clouds beyond the solar circle the change in Figure 3*a* would probably have been quite small, confined mainly to the distant ridge subtracted in Figure 3*b*. Figure 3*a* is the most direct way to compare CO molecular clouds with continuum radio, IR, and gamma-ray surveys and is the form in which the present survey was used to study the relation of molecular clouds in the first quadrant to the high-energy gamma rays observed by *COS B* (see § IV).

A prominent feature of Figure 3*a* is the intense central ridge of CO emission $\sim 2°$ thick at longitudes less than 45°. This dense concentration of molecular clouds in the distant Scutum and 4 kpc arms has been called the molecular ring on the assumption that it represents an axisymmetric distribution of clouds with respect to the galactic center. To remove this distant CO emission and display the local clouds better, the velocity integration in Figure 3*b* was limited to the interval -10 to $+20$ km s^{-1}. Figure 4 (Plate 15) is a slightly different version of this map (integrated -10 to 34 km s^{-1}) compared with the Mount Wilson photographic mosaic of the Milky Way. The upper velocity limit of 34 km s^{-1} was chosen in order to include in the map all major clouds that contribute to the obscuration of the Great Rift. It is obvious from the comparison that the correlation between the low-velocity CO emission and the Great Rift obscuration is remarkably good. Nearly every dark nebula is a molecular cloud, and vice versa. Two large components of the Rift are especially prominent, one corresponding to the Aquila Rift between longitudes 20° and 40° and another to the Cygnus Rift between 65° and 85° (Fig. 3*c*).

Figure 5 gives two longitude-velocity diagrams of the survey that differ in range of latitude, velocity smoothing, and contour interval, and, for comparison, a third similar diagram from what we call the deep survey, the Goddard-Columbia CO survey of the galactic plane covering $\pm 1°$ in latitude at 8′ resolution (Cohen *et al.* 1980; Cohen, Dame, and Thaddeus 1985). In Figure 5*a* essentially all the molecular gas detected in the present survey is displayed at fairly high velocity resolution: 2 km s^{-1}. The latitude integration extends over the full range of the survey at velocities below $+20$ km s^{-1}, but above that it is limited to the inner $\pm 2.^{\circ}5$ since almost no high-velocity molecular gas exists farther from the plane. As a result of this difference the instrumental noise, which increases as the square root of the latitude range, below 20 km s^{-1} is higher by a factor of nearly 2 than above. The linear contour interval, 1.75 K times degrees galactic latitude (K deg), chosen just to reach the noise peaks below $+20$ km s^{-1} on the left of the figure, is well above the noise on the right, so Figure 5*a* does not adequately bring out the distant clouds in the inner galaxy.

To display these distant clouds better and to facilitate comparison with the deep survey, the latitude integration in Figure 5*b* was limited at all velocities to $\pm 2.^{\circ}5$, the spectra further

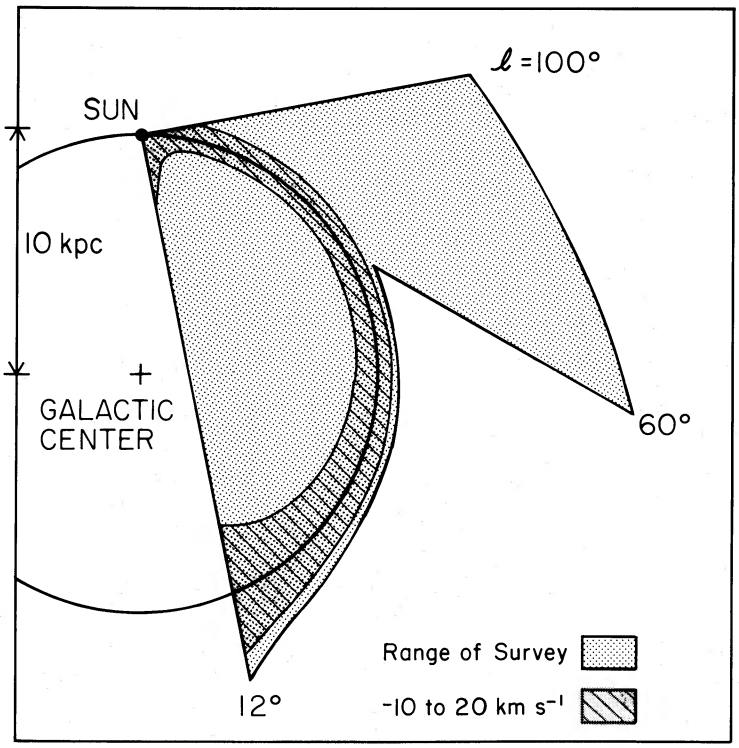

FIG. 2.—Region of the galaxy surveyed at latitudes within 3° of the plane, as well as the region corresponding to the range of velocity integration in Fig. 3*b*: -10 to $+20$ km s^{-1}. Transformation of radial velocity to distance is based on Burton's (1971) rotation curve for the inner galaxy, a radius of 10 kpc for the solar circle, and a flat rotation curve ($\theta = 250$ km s^{-1}) beyond.

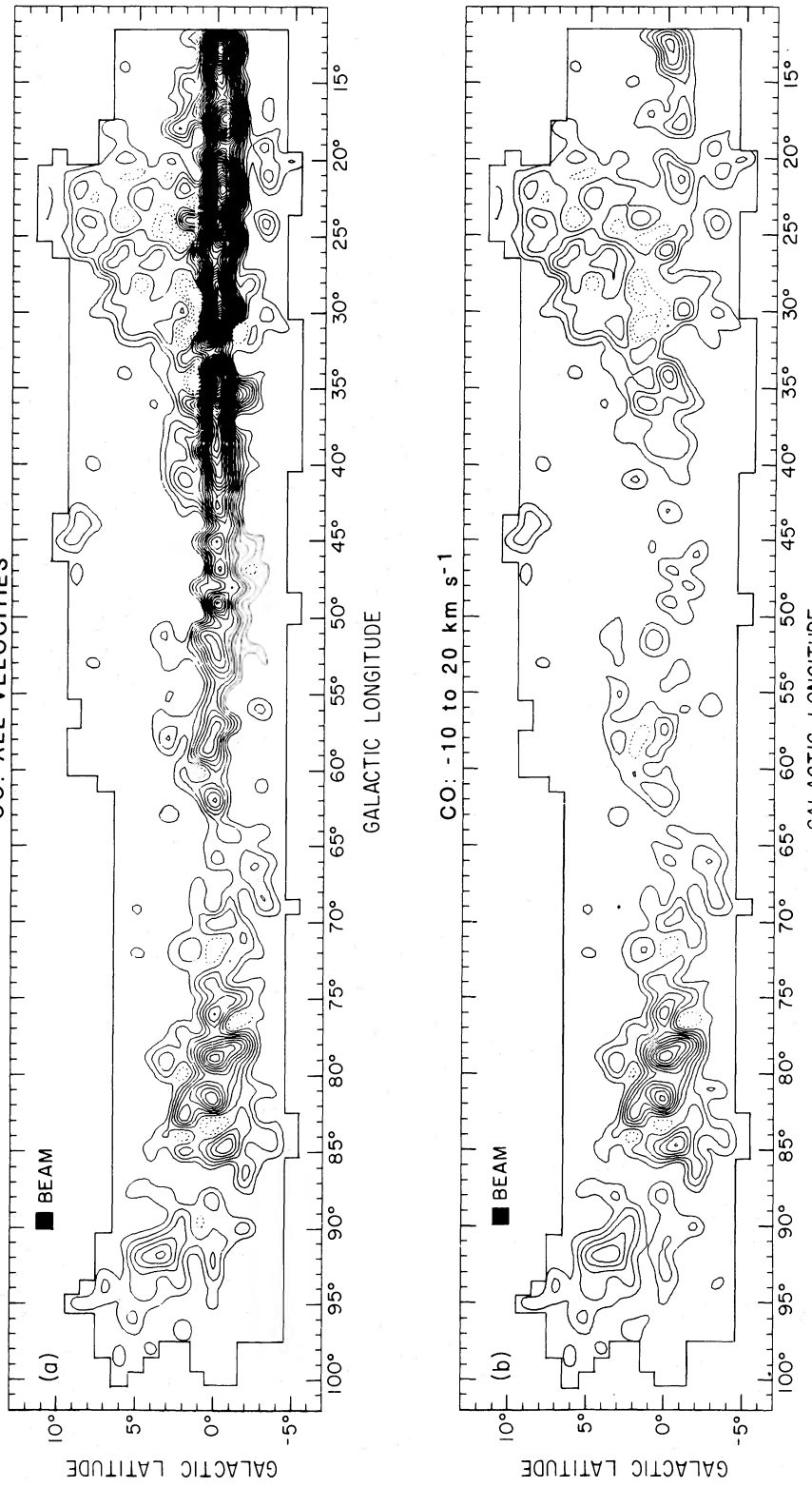

FIG. 3.—Maps of velocity-integrated CO emission from the present survey, with an H I 21 cm map for comparison. (*a*) CO data when the velocity integration covers the full 166 km s^{-1} of the spectrometer, corresponding to the region of the galactic plane shown in Fig. 2; the contour interval is 4 K km s^{-1}. (*b*) Contour interval is the same, but the velocity integration is restricted to local material: −10 to +20 km s^{-1}. (*c*) Most conspicuous local molecular clouds and the location of the OFF positions used for position switching. (*d*) Velocity integrated 21 cm map of the same region, derived from the Berkeley low-latitude survey. Contour interval is 500 K km s^{-1}.

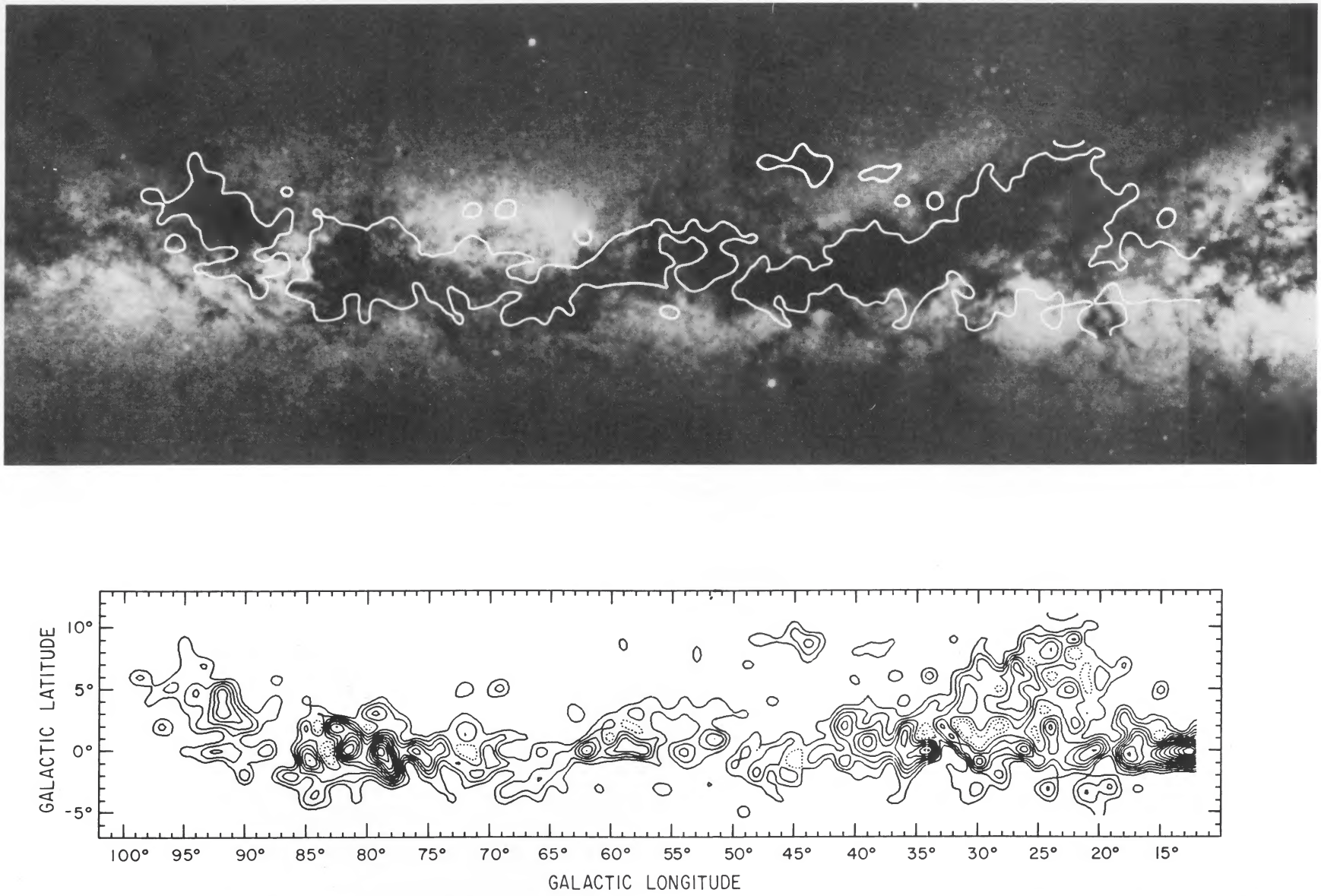

FIG. 4.—Mt. Wilson mosaic of the Milky Way from Sagittarius to Cassiopeia compared with a contour map on the same scale of the CO emission integrated between -10 and 34 km s^{-1}. Mosaic is a composite of four photographs obtained by W. C. Miller in 1957–1959 with a 5″ Ross lens at f5.6 on IIa-D emulsions (Bedke 1985). CO contour interval is 4 K km s^{-1}; the lowest contour is overlaid on the mosaic.

DAME AND THADDEUS (*see* page 754)

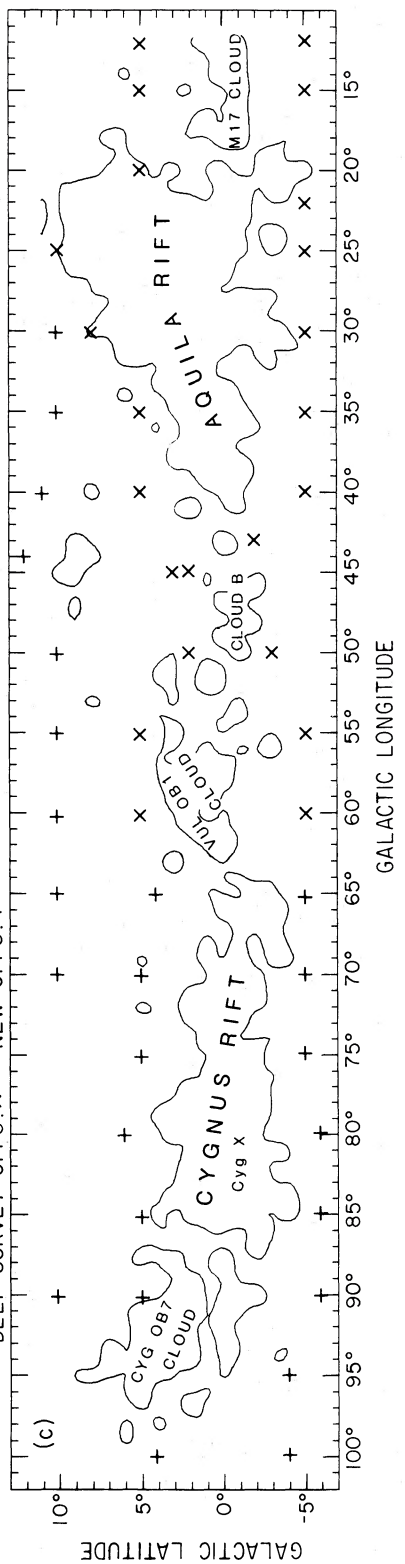

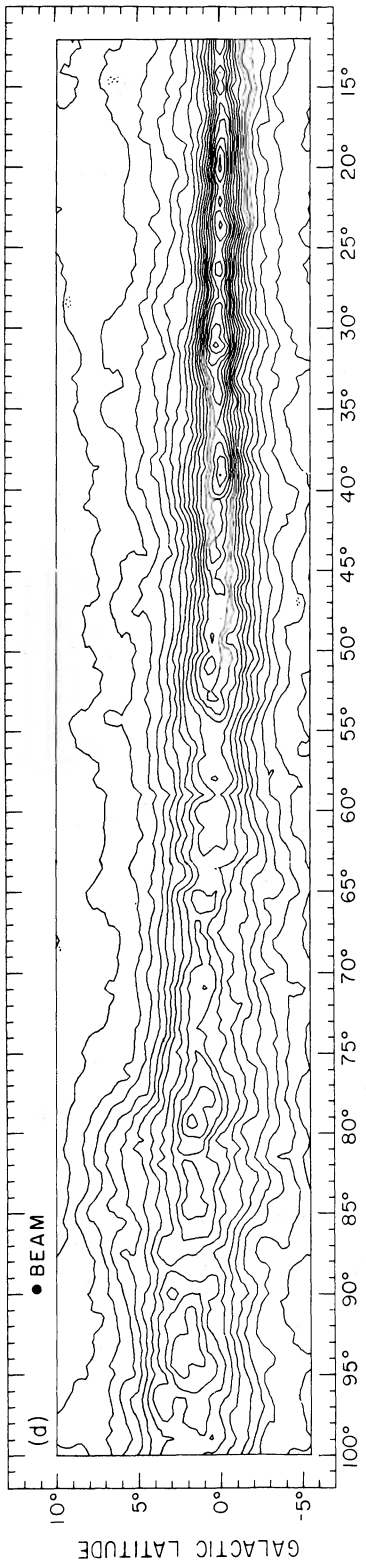

FIG. 3—*Continued*

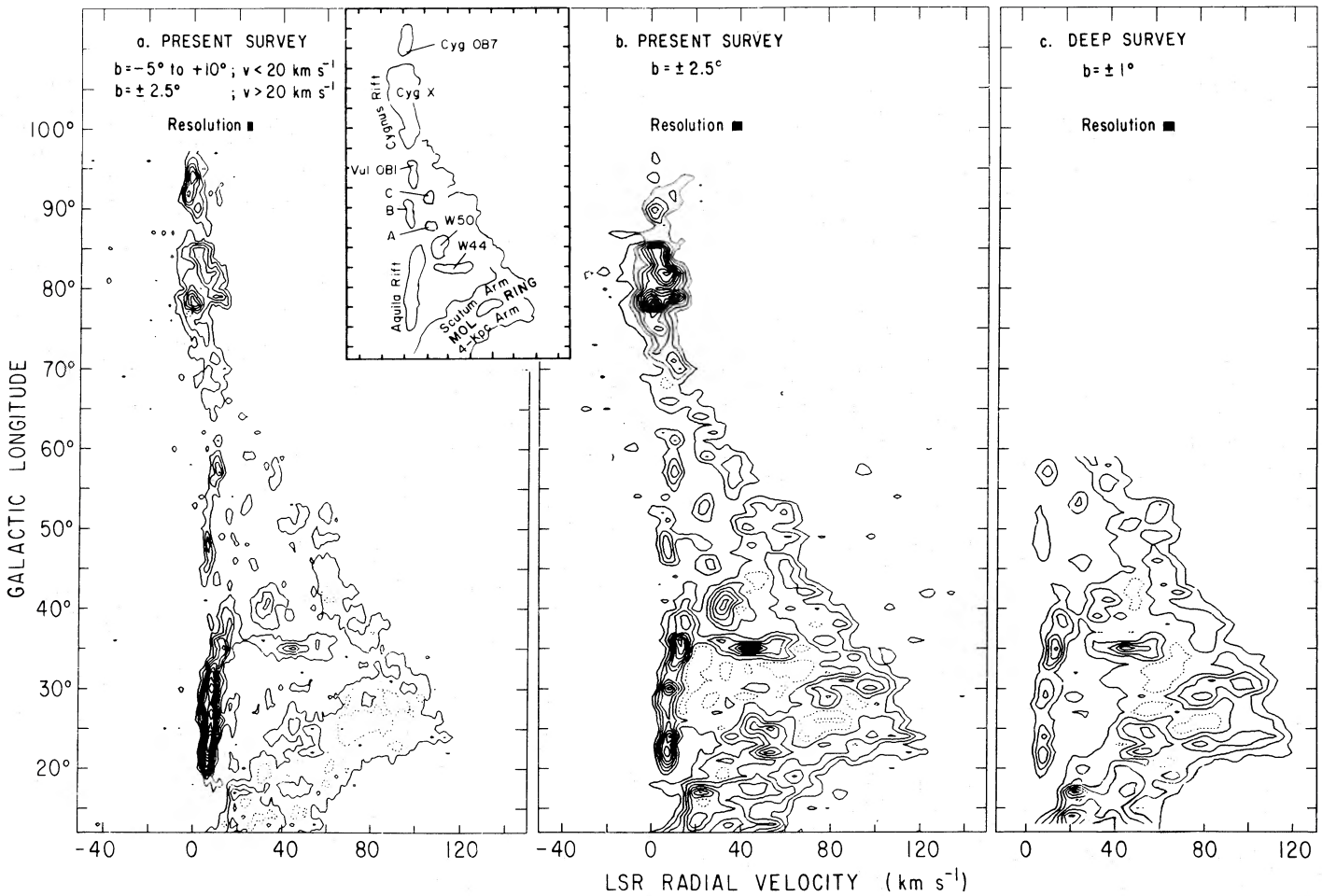

FIG. 5.—Longitude-velocity diagram of the present survey, compared with that from the deep Columbia survey of the inner first quadrant. (*a*) Diagram for all molecular clouds observed in the present survey, slightly smoothed in velocity (to a resolution of 2 km s^{-1}) to suppress noise. Contour interval is 1.75 K deg. Since at velocities above 20 km s^{-1} there is almost no molecular gas more than 2°.5 from the plane, the integration over *b* has been limited to this range; consequently, the noise level is lower above 20 km s^{-1} than below. To bring out the distant molecular clouds of the inner galaxy, and, for comparison with the deep Columbia survey, (*b*) is the survey integrated over $b = \pm 2°.5$ at all velocities, further smoothed in *v* (to a resolution of 5.2 km s^{-1}) and taken to a lower contour level: 0.75 K deg. (*c*) Deep survey integrated over its full latitude range of ±1°, boxcar-smoothed to an angular resolution of 1°, and contoured exactly as in (*b*). As discussed in the text, and shown by Fig. 6, the small differences between (*b*) and (*c*) can be attributed almost entirely to the wider latitude coverage of (*b*).

smoothed in velocity to a resolution of 5.2 km s^{-1}, and the contour interval reduced by a factor of 2.3 to 0.75 K deg. The most conspicuous large molecular complexes in the inner galaxy, including those associated with the radio continuum sources W44 and W50, are now easily identified (Fig. 5 insert), even though the present survey represents over an order of magnitude less observing time per unit solid angle than the deep survey.

In Figure 5*c* the deep survey is shown smoothed to the same velocity and longitude resolution as Figure 5*b* and contoured to the same level. The qualitative and quantitative agreement between the two is striking; the slight differences can be attributed almost entirely to diffuse nearby clouds, such as the Aquila Rift, or to large molecular complexes in the near Sagittarius Arm, such as those associated with W44 and W50, which extend more than 1° from the galactic plane and were somewhat clipped by the deep survey.

For the best possible quantitative comparison of the two surveys, the contribution to Figure 5*b* of material more than 1°.5 from the plane has been subtracted (i.e., only spectra taken at $b = 0, \pm 1°$ retained), and both surveys were integrated over radial velocity. The result (Fig. 6) shows little instrumental noise; the jagged peaks are almost entirely real, the effect of clumpiness and statistical fluctuation in the molecular clouds along the plane; the slight differences between the two surveys can again be largely attributed to the difference in latitude coverage, here amounting to only 0°.5. Since the present survey and the Columbia deep survey are entirely independent, this agreement represents an extremely stringent check on their respective calibrations, sampling, and data analysis. To our knowledge, no other large-scale spectral line survey of the galaxy has been subjected to such a rigorous quantitative check.

IV. THE H_2-TO-CO RATIO

An important by-product of the present survey is a new calibration of CO as a mass tracer for molecular clouds which is superior in several respects to previous calibrations from star counts or the virial theorem. This new method, based on an intercomparison of our CO data, the Berkeley 21 cm survey, and the *COS B* survey of high-energy diffuse galactic gamma-rays, was recently discussed in detail by Lebrun *et al.* (1983)

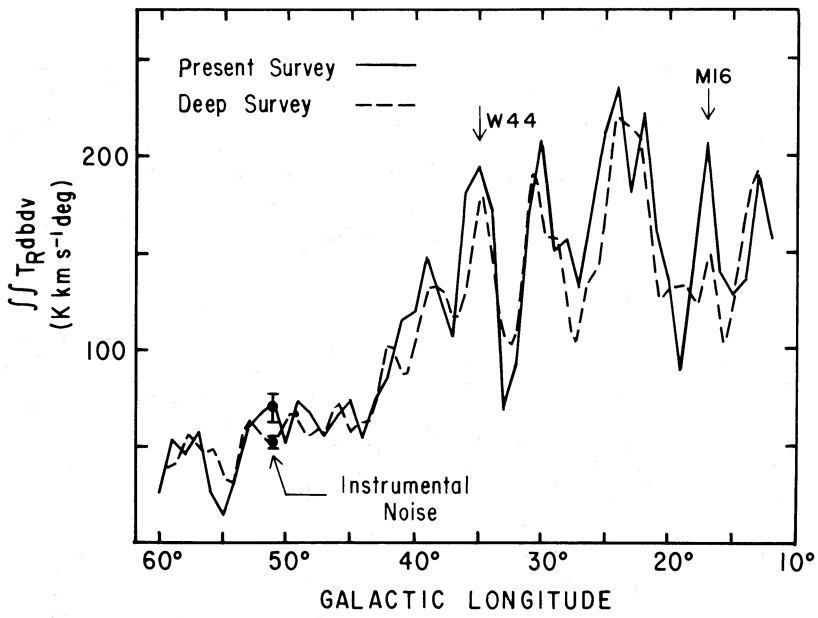

FIG. 6.—Numerical integration of the survey over $\pm 1\overset{\circ}{.}5$ in galactic latitude and over all velocities (*solid line*), compared with a similar curve (*dashed line*) derived from the Columbia deep survey, integrated over its full latitude range of $\pm 1°$ and smoothed in l to a resolution of 1°. M16 and W44 are large molecular clouds which extend beyond the latitude limits of the deep survey.

and Bloemen *et al.* (1984, 1985). Here we only summarize the basic procedure, state the result, viz., the ratio of the H_2 column density to the velocity integrated intensity of the CO $1 \rightarrow 0$ line, $N(H_2)/W_{CO}$, and show that it is in reasonable agreement with spectroscopic estimates from background stars of the extinction in the Aquila Rift.

The fundamental assumption on which the method is based is that the CO $1 \rightarrow 0$ line is not only a good qualitative tracer of the unobserved H_2 and He which presumably constitute most of the mass of molecular clouds—a proposition accepted by all molecular cloud observers—but also a good quantitative one *when averaged over a suitably large area.* This assumption is neither self-evident, since the $1 \rightarrow 0$ line is often optically thick in molecular clouds, nor yet adequately justified theoretically, although it is currently the basis of most estimates of the mass of molecular clouds here and in other galaxies. Its justification is entirely empirical: the finding by many observers that the $1 \rightarrow 0$ line profiles of the rare isotopic species of CO, especially ^{13}CO, are generally proportional to the profile of the normal species when averaged over a cloud or even a fairly small portion of a cloud (e.g., Kutner *et al.* 1977). The $^{13}CO/CO$ intensity ratio is typically one-fourth. If, as generally believed, the rare isotopic species of CO are the best available tracers of mass in molecular clouds, it must follow that the normal species too is a mass tracer: the important point is to determine the correct constant of proportionality, which is what the gamma-ray comparison does.

A second fundamental assumption is that the observed high-energy ($E > 300$ MeV) gamma-ray flux is directly proportional to the total gas density along the line of sight. Further, it is assumed that these gamma rays result mainly from the interaction of cosmic rays with the interstellar gas through the decay of π° mesons and that the cosmic-ray density in the galaxy is uniform, i.e., that cosmic rays readily penetrate molecular clouds, so the gamma-ray emissivity per gas nucleon is the same within the clouds as without.

Lebrun *et al.* show that the observed gamma-ray emission, omitting isotropic background counts, can then be expressed as

$$I_\gamma = AN(\text{H I}) + BW_{CO} ,$$

where N(H I) is the atomic column density, derived from 21 cm surveys (Fig. 3*d*), and W_{CO} the velocity-integrated CO emission (Fig. 3*a*). The ratio of A and B, which are free parameters adjusted to fit the observed gamma-ray distribution on the plane of the sky, yields the H_2-to-CO ratio: $N(H_2)/W_{CO} = B/2A = 3 \times 10^{20}$ cm^{-2} K^{-1} km^{-1} s. Lebrun *et al.* then argue that this is the upper limit, since either a galactic cosmic-ray gradient or a substantial contribution from gamma-ray point sources would decrease the ratio. They obtained a lower limit of 1×10^{20} cm^{-2} K^{-1} km^{-1} s by estimating the maximum possible contribution from gamma-ray point sources and showed that this agreed with independent estimates of a lower limit of the ratio from extinction measurements in dark clouds.

Because of the possibility of a metallicity gradient in the Galaxy, it would not be surprising to find that $N(H_2)/W_{CO}$ depended on galactocentric distance R, and, in particular, to find that in the molecular ring the ratio was significantly *lower* than locally owing to a greater abundance there of C and O. As Figure 7 shows, the CO emission detected by the present survey comes nearly equally from local clouds, mainly in the Great Rift system, and from distant clouds in the ring, so the calibration of Lebrun *et al.* is a hybrid which should be compared with a purely local calibration in order to sort out the separate contributions from near and far material. This was done by Bloemen *et al.* (1984), who compared the Columbia CO survey of the extensive complex of molecular clouds in Orion and Monoceros (Thaddeus 1982; Maddalena *et al.* 1985) with the *COS B* survey of the same region and obtained $N(H_2)/W_{CO} = 2.6 \pm 1.2 \times 10^{20}$ cm^{-2} K^{-1} km^{-1} s, in good agreement with the determination by Lebrun *et al.* There is therefore no evidence for a large difference in the H_2-to-CO ratio between the molecular ring and the solar circle.

This conclusion was recently strengthened by Bloemen *et al.*

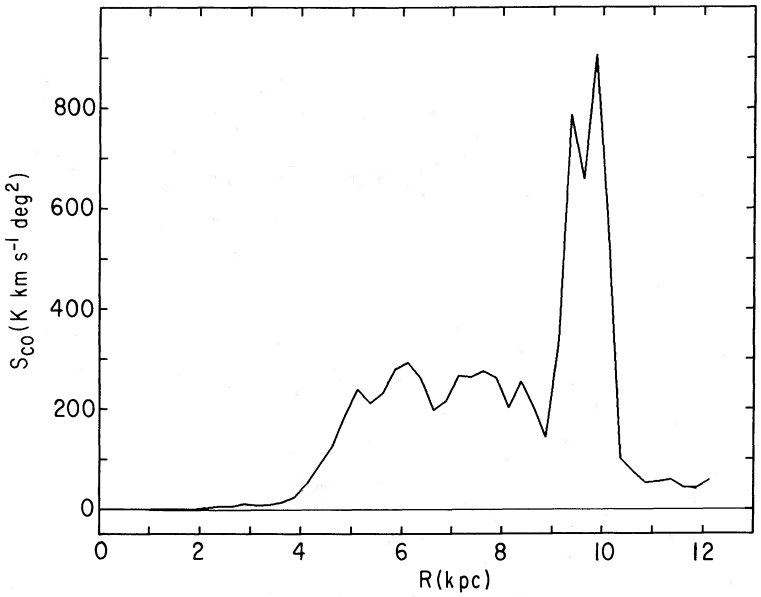

FIG. 7.—Apparent CO brightness of 250 pc wide galactic radius bins. Graph was produced by adding the emission in each spectral channel of the survey into a kinematically assigned radius bin and multiplying these sums by the survey sampling intervals in l, b, and v ($1° \times 1° \times 0.65$ km s^{-1}). Graph indicates the amount of emission contributed to the survey by material at each galactic radius.

(1985) by a reanalysis of the present survey with more complete *COS B* data and with more extensive Columbia CO data in the second quadrant from New York as well as in the third quadrant from Chile. In units of 10^{20} cm^{-2} K^{-1} km^{-1} s, they find for $R = 2$–8 kpc that $N(H_2)/W_{CO} = 2.8 \pm 0.7$ and for $R > 8$ kpc the same value to within the statistical uncertainty: $N(H_2)/W_{CO} = 2.7 \pm 0.4$. In the following discussion we adopt the latter ratio for local material.

Another demonstration of the large contribution of local material to the observed galactic CO emission is provided by Figure 8. The lower curve is an integration over all velocities and over $\pm 1°.5$ in latitude, while the upper curve extends the latitude integration over the full range of the survey. Because of their large angular sizes, the major components of the Great Rift, e.g., the Aquila Rift ($l = 20°$–$40°$), the Cygnus Rift (70°–87°), and the Cyg OB7 molecular cloud (88°–96°), contribute substantially to the overall emission, and in low angular resolution continuum surveys they tend to be confused with background objects. The Aquila Rift, in particular, lies toward the molecular ring and seems to have caused several groups (e.g., Stecher *et al.* 1975; Cesarsky, Cassé, and Paul 1977) to overestimate the density of molecular gas and cosmic rays in the ring. These early investigations of the galactic gamma-ray emission relied on the *SAS 2* gamma-ray data (Fichtel *et al.*

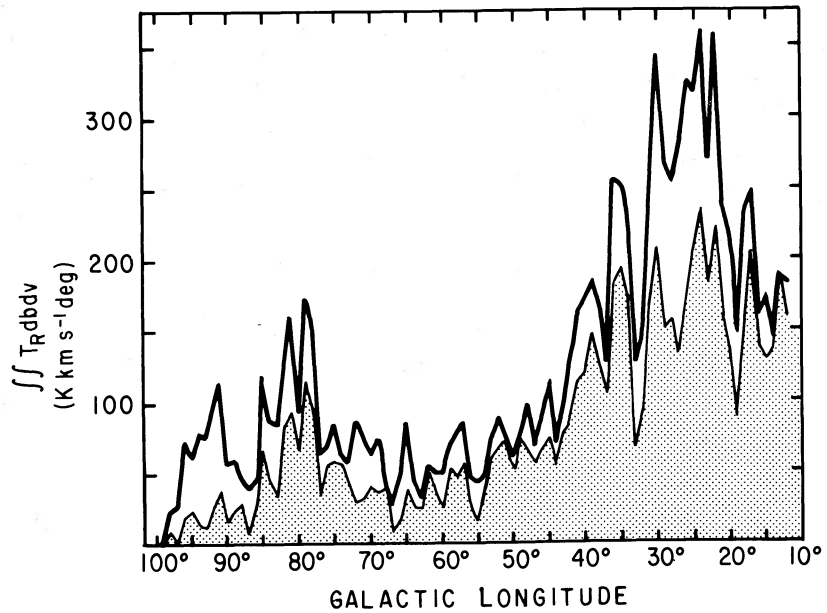

FIG. 8.—Longitude profiles of the survey integrated over all velocities and over latitude. The lower line (*light*) is integrated over $\pm 1°.5$ in latitude, while the upper line (*heavy*) is over all latitudes covered by the survey.

1975) and the galactic plane CO surveys of Scoville and Solomon (1975) or Gordon and Burton (1976), which were all used in the form of longitude profiles, like those in Figure 8. Because of the low sensitivity of the *SAS 2* survey, the gamma rays were summed over $\pm 10°$ in latitude to obtain adequate statistics and so contained a substantial contribution from the Aquila Rift, but the CO surveys, confined to the galactic plane, contained little. As a result, the gamma-ray emissivity of the inner galaxy was overestimated. The high emissivity was attributed to a very high molecular gas density in the inner galaxy or to an enhancement of cosmic rays in that region, or to a combination of both. Lebrun *et al.* (1983) avoided this problem by using the *COS B* gamma-ray survey, which has better counting statistics, and performing the analysis over the full latitude range of our CO survey.

The Aquila Rift is not a highly opaque molecular cloud; its mean visual extinction is only of the order of 2 mag, and distant O stars are observed through it. The spectroscopically determined extinction along the line of sight to these stars can be used to check the gamma-ray calibration of the $N(H_2)/W_{CO}$ ratio. Nine of the O stars in the catalog of Garmany, Conti, and Chiosi (1982) lie in directions where significant CO emission is detected; these are tabulated in Table 3, with distances, visual extinctions, and other data from the same article. To obtain the extinction from the Aquila Rift itself, correction must be made for the extinction from the diffuse 21 cm gas along the line of sight. To do so, the H I column density to the star was computed by adopting a mean midplane H I density of 0.35 cm^{-3} and a scale height of 130 pc (Burton 1976); the visual extinction from the H I (col. [8], Table 3) was then derived taking $A_V/E(B-V) = 3$ and $N_H/E(B-V) = 5.8 \times 10^{21}$ atoms cm^{-2} mag^{-1} (Bohlin, Savage, and Drake 1978), where N_H is the total hydrogen column density and $E(B-V)$ the color excess.

On the assumption that the same "gas-to-dust" ratio holds for the molecular gas of the Aquila Rift, we then obtain the H_2 column densities in column (9) of Table 3, and, from our CO survey data in column (10), the ratio $N(H_2)/W_{CO}$ in the last column. There is too much scatter in the results to obtain a value for the ratio that is very accurate statistically, but the average values obtained agree well with that derived from the gamma-ray comparison: in units of 10^{20} cm^{-2} K^{-1} km^{-1} s, the mean ratio from all nine stars is 2.5 ± 1.6, and that for the four within 3 kpc is 3.6 ± 1.6; the ratio of the total H_2 column density to the total integrated CO emission toward all nine stars is 2.2. All are therefore in satisfactory agreement with our adopted value from the gamma-ray analysis.

V. THE GREAT RIFT SYSTEM OF MOLECULAR CLOUDS

We have seen that the vertical lane of CO emission that runs through our CO *l*, *v* map near $+10$ km s^{-1} (Fig. 5) arises from molecular clouds forming the Great Rift in the Milky Way (Fig. 4). This lane is the molecular counterpart of a very extended 21 cm feature, Lindblad's (1967) feature A, present in all four galactic quadrants. Like the CO emission, feature A has a very wide latitude extent and small velocity dispersion, and both in absorption at low latitudes against the distant inner disk and in emission at higher latitudes its velocity coincides closely with that of the CO. Lindblad *et al.* (1973) interpreted feature A as an expanding ring of gas surrounding the Sun and suggested it may be related to young stars in Gould's Belt and the dust clouds of the Great Rift, but this connection could not be clearly established with the 21 cm data alone. The connection is firmly established by our CO survey. The close correspondence between the CO emission and the optical obscuration (Fig. 4) implies that feature A, or at least the molecular counterpart of feature A, does indeed arise from the Gould Belt population of dark clouds forming the Great Rift.

The nature of the Great Rift is a longstanding problem. There have been several recent attempts to resolve the Rift into regions of roughly uniform obscuration, on the assumption that each such region corresponds to a distinct dust cloud at a particular distance (e.g., Neckel and Klare 1980). Using our CO survey, it is a simple matter to resolve the Rift into discrete molecular clouds, since even clouds which overlap in direction are generally well resolved in radial velocity (Fig. 5). The Rift is decomposed into its individual molecular clouds in Figure 9. Distances were determined kinematically (for some of the more distant clouds), or with the aid of associated Population I objects, or from the relation of visual absorption versus distance for stars within the cloud boundaries (e.g., Forbes 1985). A discussion of the distance determination for each cloud and other details are given in the Appendix.

The cloud distances as well as other important observational parameters are given in Table 4. The mean velocities, line widths, and apparent CO luminosities (S_{CO}) were determined by fitting Gaussians to the clouds' composite line profiles, produced by averaging all spectra within the cloud boundaries shown in Figure 9; all except M17 (see Appendix) were roughly Gaussian in shape. The cloud radius was defined as $(A/\pi)^{1/2}$, where A is the cloud's linear projected area, computed from the distance and apparent area in Table 4. The cloud mass M_{CO} was computed directly from its apparent CO luminosity and distance with our standard conversion factor $N(H_2)/W_{CO} = 2.7$

TABLE 3

O STARS BEHIND AQUILA RIFT

Star (1)	l (2)	b (3)	Spectral Type (4)	V (mag) (5)	Distance (kpc) (6)	A_v (mag) (7)	A_v(H I) (mag) (8)	N_{H_2} (10^{20} cm^{-2}) (9)	W_{CO} (K km s^{-1}) (10)	N_{H_2}/W_{CO} (10^{20} cm^{-2} K^{-1} km^{-1} s) (11)
BD −11 4674	21°0	−1°2	O9.5 I	10.18	3.4	4.22	1.76	23.7	12.3	1.9
BD −08 4617	22.8	1.0	O8.5 V	9.36	1.0	3.66	0.50	30.5	5.9	5.2
HD 173010	23.7	−2.5	O9.5 I	9.18	3.2	3.35	1.48	18.0	5.5	3.3
BD −08 4634	23.8	0.1	O9 V	9.44	1.0	3.64	0.50	30.3	6.5	4.7
HD 173783	24.2	−3.3	O9 I	9.31	5.2	2.43	1.53	8.7	9.7	0.9
HD 172175	24.5	−0.8	O6 F	9.44	3.6	2.96	1.96	9.6	8.4	1.1
HD 172275	25.0	−0.7	O6	9.35	1.8	3.37	1.00	22.9	9.4	2.4
BD −04 4503	26.8	1.3	O7	10.83	2.9	3.32	1.53	17.3	9.2	1.9
BD −05 4769	27.7	−1.8	O8 I	10.40	5.7	3.32	2.38	8.1	8.6	0.9

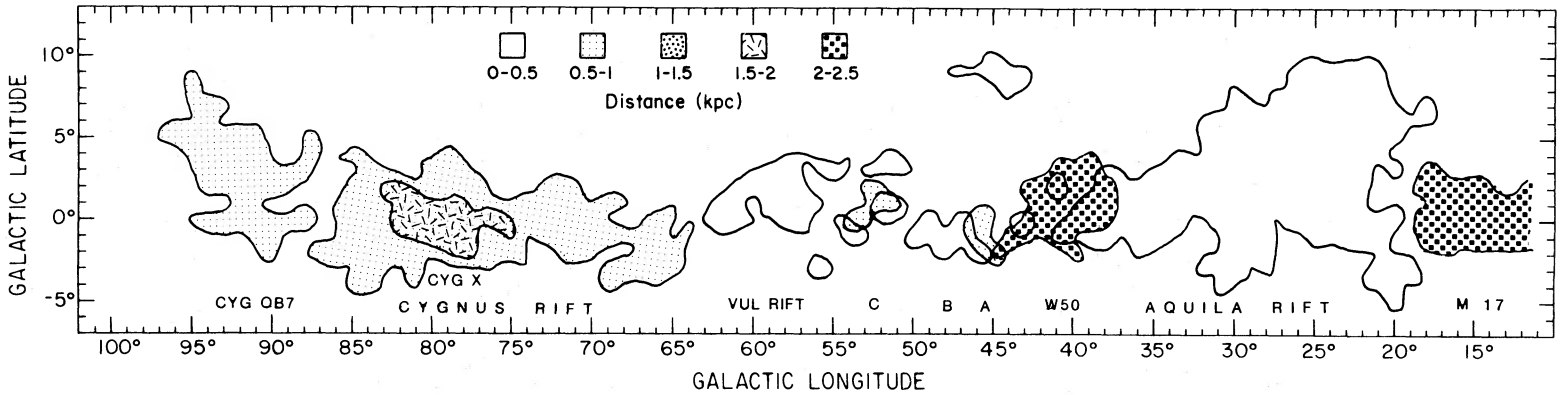

FIG. 9.—Schematic map of the individual molecular clouds which comprise the Great Rift. Cygnus X is defined by its 12 K km s^{-1} CO contour, the rest by their 4 K km s^{-1} contours. Distances are indicated by the shading.

TABLE 4

OBSERVATIONAL CLOUD PARAMETERS

Cloud	V_{LSR} (km s^{-1})	Δv (FWHM) (km s^{-1})	Area (deg^2)	S_{CO} (K km s^{-1} deg^2)	Distance (kpc)	Notes	Radius (pc)	M_{CO} (10^5 $M_\odot$)	M_{vir} (10^5 $M_\odot$)
M17	21	10	17	240	2.3	1	93	23	20
Aql Rift	8	7	162	1566	0.2	2	25	1.1	2.6
W50	32	10	26	209	2.2	3	110	18	23
Cloud A	27	4	8	21	0.5	2	14	0.10	0.47
Cloud B	7	4	9	67	0.3	2	9	0.11	0.29
Cloud C	24	5	10	47	0.5	2	16	0.21	0.84
Vul Rift	10	4	21	133	0.4	2	18	0.39	0.60
Cyg Rift	7	13	111	1046	0.7	2	73	9.3	26
Cyg X	2	15	44	969	1.7	4	111	51	52
Cyg OB7	−1	7	45	380	0.8	1	53	4.4	5.5

NOTES.—(1) Spectroscopic distance to related OB association or stellar cluster. (2) Discontinuity in A_v with distance: Neckel and Klare 1980. (3) Near kinematic distance (Burton 1971). (4) Cong 1977.

$\times 10^{20}$ cm^{-2} K^{-1} km^{-1} s and a mean molecular weight per H_2 molecule of $2.76m_H$. Table 4 also gives virial masses, computed from the line widths and radii by approximating the clouds as uniform density spheres in virial equilibrium:

$$M_{vir} = \frac{5}{8G \ln 2} R\Delta V^2 ,$$

where G is the gravitational constant, R the radius of the cloud, and ΔV its full line width at half-intensity.

The characteristics of the Great Rift molecular clouds (Table 4) vary greatly, ranging over more than an order of magnitude in distance and radius and over more than two orders of magnitude in mass. To judge from the other Columbia surveys of more distant clouds both within the solar circle and without, these appear a fairly typical sample of molecular clouds in the Milky Way. Most seem to be close to virial equilibrium (Table 4), the average ratio of virial mass to estimated mass being 2.2 ± 1.3, and follow closely the relation between radius and line width derived by Dame *et al.* (1985) from a larger sample of clouds in the first quadrant (Fig. 10). This $R - \Delta V$ relation can be used with the observed line width and angular radius of a cloud to estimate its distance directly; although the scatter of the relation (Dame *et al.* 1985) makes this distance somewhat uncertain, it is sometimes adequate to distinguish between two possible distances (e.g., between the near and far kinematic distances; see Appendix).

The most prominent component of the Great Rift system of dark clouds is the Aquila Rift, the large lane of obscuration between $l = 20°$ and 40° apparently produced by a single cloud that contains $\sim 1 \times 10^5$ $M_\odot$ of molecular gas at a distance of ~ 150 pc. This cloud is probably related to both the ρ Oph molecular cloud (Myers *et al.* 1978) and the very extended, cold

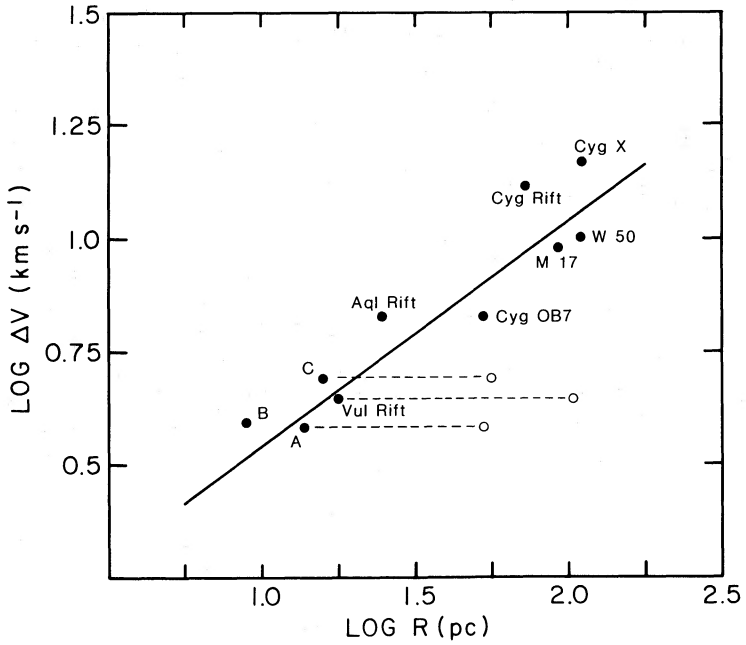

FIG. 10.—Logarithm of the line width ΔV (FWHM) of each cloud listed in Table 4, plotted against the logarithm of its radius R. Open circles indicate the positions of clouds A and C if they lie at the near kinematic distances of ~ 2 kpc and of the Vul Rift if it lies at the distance of the Vul OB1 association, 2.3 kpc. Straight line is not a fit to the points; it was taken from the analysis of inner galaxy clouds by Dame *et al.* (1985) and is given by the equation $\log \Delta V = 0.08 + 0.50 \log R$.

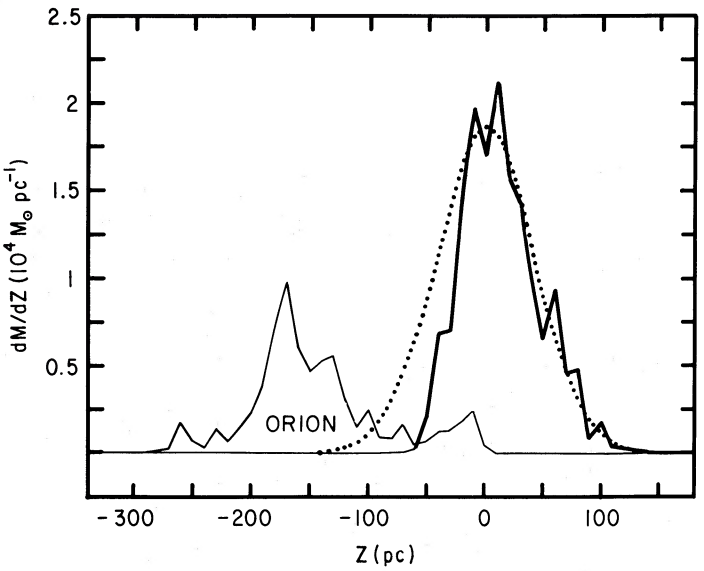

FIG. 11.—The mass distribution with respect to distance from the galactic plane z of the clouds in Table 4 with distances < 1 kpc (*heavy line*) and of the clouds in the Orion-Monoceros region mapped by Maddalena *et al.* (1985) (*light line*). Integrated CO intensity W_{CO} was converted to mass (see § IV) for each point in each cloud and added into 10 pc wide bins in z. Dotted curve is a Gaussian fit to the positive-latitude data (*heavy line* at $z \geq 0°$); it has a peak of $1.9 \times 10^4\ M_\odot\ pc^{-1}$ and a width (FWHM) of 100 ± 12 pc.

H I cloud seen as an H I self-absorption feature in the region from $l = 345°$ through the galactic center to $l = 25°$, at $|b| < 10°$ (first detected by Heeschen 1955; later mapped by Riegel and Crutcher 1972; Crutcher and Lien 1985). A connection to ρ Oph was established by Lebrun and Huang (1984), who found fairly extensive CO emission linking the two clouds spatially and in velocity; the connection is not surprising, since the clouds are joined by heavy optical obscuration (partly seen in Fig. 4 extending toward the upper right from the Aquila Rift). The Aquila Rift and the cold H I cloud are comparable in angular size, are similarly displaced to positive latitude, and have similar velocities and narrow line widths; they are estimated to be at nearly the same distance and partially overlap spatially in the region $l = 20°$ to 25°. The Aquila Rift and ρ Oph molecular clouds and the cold H I cloud may therefore comprise a single large lane of cold gas which extends over 55° of galactic longitude, corresponding to a linear size of 140 pc. The lane itself may be just a small part of the expanding ring of Lindblad *et al.* (1973).

VI. HALF-THICKNESS AND DENSITY OF LOCAL MOLECULAR GAS

With distances in hand, an estimate of the thickness of the local population of molecular clouds and the mean local density of molecular gas can now be made. Besides being of interest to studies of galactic structure, these parameters may be relevant to understanding the evolution of the comet cloud of the solar system, and, therefore, even events in the geological and biological record. Rampino and Stothers (1984), for example, have suggested that encounters with molecular clouds as the solar system oscillates about the galactic plane are the cause of a claimed 30 Myr periodicity in the occurrence of large impact craters and biological extinctions on Earth; they propose that such encounters perturb the solar system's cloud of comets, sending many into the inner solar system where one or more collide with the Earth. Thaddeus and Chanan (1985) have shown that the ratio of the amplitude of the solar oscillation (72 pc) to the thickness of the molecular disk is the parameter crucial to this hypothesis, and they find that with the mean half-thickness at the solar circle, 85 ± 20 pc, derived from the deep Columbia CO surveys, no statistically significant period can be extracted from the small number of well-dated episodes of biological extinctions or impact craters. To check their conclusion, it is clearly desirable to estimate the thickness of the molecular cloud disk from *purely local* observations such as those here.

We will define as local those molecular clouds in Table 4 within 1 kpc of the Sun. We assume, as before (see Appendix), that the Cygnus Rift extends through the Cygnus X region with a CO intensity equal to its average intensity below $l = 74°$. The heavy line in Figure 11, then, is the distribution with respect to distance from the galactic plane z of the molecular gas in these objects, obtained simply by numerical integration of the spectra from our survey, with latitude converted to z with the distances in Table 4. The half-width at half-intensity of the Gaussian that fits this profile is 40 pc, but this width is somewhat biased by the asymmetry of our survey, which typically extends 3° farther from the galactic plane to positive latitude than to negative latitude. A less biased value is obtained by fitting only the positive latitude data, resulting in a fit, shown in Figure 11, that has a half-thickness of 50 pc.

It is likely that inclusion of local material in the three quadrants not covered by our survey would increase this thickness somewhat—probably by a few tens of parsecs. The reason, as can readily be seen from the dark cloud surveys of Lynds (1962) and Feitzinger and Stuewe (1985), is that we surveyed few of the many high-latitude clouds in Gould's Belt, e.g., the clouds 10°–25° off the galactic plane in Ophiuchus, Taurus, or Orion. The z distribution of the very extensive cloud complex associated with the Orion Nebula, NGC 2023, and NGC 2068 (Maddalena *et al.* 1985), containing a significant fraction of local molecular gas by mass, is shown by the light line in Figure 11. We can roughly estimate the influence of Orion on the half-thickness by scaling our first quadrant latitude profile (*heavy line*) by a factor of 4, to account for the other three quadrants, and then adding the Orion profile. It is evident from Figure 11 that the resultant profile cannot be properly fitted by a Gaussian, so we computed the rms dispersion about $z = 0°$, which is 64 pc. Since inclusion of all the high-latitude Gould's Belt clouds would probably result in an even larger dispersion, as well as a latitude profile closer to a Gaussian, we conclude that 50 pc is only a lower limit to the half-thickness of the local distribution of molecular clouds, and we estimate, with a fairly large uncertainty of ± 25 pc, the true value to be 75 pc, the Gaussian half-thickness corresponding to a dispersion of 64 pc. This value agrees well with results of the deep surveys of Dame (1984) and Sanders, Solomon, and Scoville (1984) extended to the solar circle and with the value derived by Thaddeus and Chanan.

An estimate of the local density of molecular gas can now be computed directly from the cloud masses given in Table 4. The total mass of clouds within 1 kpc in the quadrant observed is $1.6 \times 10^6\ M_\odot$. Assuming this mass is distributed in z with a half-thickness of 75 pc, we find a mean midplane density of $0.013\ M_\odot\ pc^{-3}$, corresponding to $0.2\ H_2\ cm^{-3}$, and a surface density of $2.0\ M_\odot\ pc^{-2}$. These values are roughly in agreement with that predicted by extrapolating the CO radial distribution of Dame (1984) to the solar circle and about a factor of 2 lower than the estimate of Sanders, Solomon, and Scoville (1984). It

is unlikely, we think, that unobserved molecular clouds at high latitude, or the extension of the local average to the three-quarters of the galactic plane not considered here, would increase the local mean density of molecular gas by more than 50%.

VII. SUMMARY AND CONCLUSIONS

1. The Great Rift system of the Milky Way consists of a small number of well-defined CO molecular clouds. The four most conspicuous are those associated with the Aquila, Vulpecula, and Cygnus Rifts, and the stellar association Cyg OB7. Comparison of our wide-latitude CO survey of the Rift system with the Mount Wilson optical mosaic photograph of the Milky Way is perhaps the best current evidence for an important generalization: All dark nebulae are molecular clouds and vice versa.

2. The masses of the nearby molecular clouds in the Rift system are not large with respect to the giant molecular cloud complexes observed elsewhere in the Galaxy. The main nearby clouds have masses between a few times $10^4\ M_\odot$ to few times $10^5\ M_\odot$ versus a few times 10^6 for the largest complexes elsewhere. The Rift system is conspicuous mainly because it is close.

3. The tangle of distant molecular clouds in the inner galaxy is conspicuous near the galactic plane at longitudes below $\sim 50°$. In overall terms, the CO emission in our survey comes nearly equally from rather local material, 10 kpc from the galactic center, and from these distant objects which lie mainly in the Scutum and 4 kpc arms (the molecular ring) 4–7 kpc from the center.

4. The half-thickness at half-intensity of the local molecular cloud layer is greater than 50 pc and is estimated to be 75 ± 25 pc, in agreement with the half-thickness at the solar circle from deep CO surveys. The mean density of molecular gas in the galactic midplane is $\sim 0.013\ M_\odot\ \mathrm{pc}^{-3}$.

We thank B. Elmegreen and G. Herbig for helpful suggestions, E. S. Palmer for help in operating and maintaining the 1.2 m telescope, A. Smith for assistance with data analysis, H. W. Babcock and J. Bedke for providing information on the Mount Wilson mosaic of the Milky Way, E. Sarot for editorial assistance, and E. Michaud for typing the manuscript.

APPENDIX

DISCUSSION OF INDIVIDUAL CLOUDS

These notes briefly describe how we determined the distance to each complex and comment, where necessary, on the individual clouds.

a) M17

Because of its large distance, this massive complex is not a prominent component of the Great Rift; we include it here because, owing to its low galactic longitude, it is conspicuous in our low-velocity CO map (Fig. 4). Dame *et al.* (1985), using the Columbia deep CO survey, resolved this feature into two large clouds at roughly the same distance. For present purposes we consider it a single object and adopt the spectroscopic distance to M17 derived by Crampton, Georgelin, and Georgelin (1978). Because the complex is immersed in a high level of background emission, determining its line width and mass is not straightforward, so we adopted the values determined from the analysis of inner-galaxy molecular clouds by Dame *et al.* (1985).

b) Aquila Rift

The various distance estimates for the dust in the Aquila Rift are in good agreement, indicating a distance ~ 200 pc. However, its distance tends to increase with longitude, ranging from ~ 150 pc near $l = 20°$ to ~ 300 pc near $l = 40°$. This tendency is consistent with the expanding ring model of Lindblad *et al.* (1973) and with the idea that the Aquila Rift is an extension of the H I absorbing sheet of cold gas seen at lower longitude by Riegel and Crutcher (1972) (§ V). The tendency is clearly seen in graphs 10, 11, and 12 of FitzGerald (1968), showing color excess versus distance for stars toward the Aquila Rift. Similar graphs from Neckel and Klare (1980) suggest a distance of ~ 250 pc; their regions 254 (centered at $l = 21°$, $b = +40°$) and 260 ($l = 30°$, $b = 0°$) cover more than half the area of the Aquila Rift. Also of note are the studies of Lucke (1978), Sherwood (1974), Krautter (1980), and Forbes (1985), which are consistent with a distance of 200 ± 100 pc.

c) W50

This is one of the most massive and distant molecular clouds visible as a dark nebula (Huang, Dame, and Thaddeus 1983). Dame *et al.* (1985) resolved it into three separate but probably related objects; for present purposes we consider it a single object and adopt the near kinematic distance, 2.2 kpc. The far kinematic distance is ruled out by the cloud's large angular size, small line width (Fig. 10), and visibility.

d) Clouds A and C

We consider these together because they are quite similar objects. Although the near kinematic distances of the clouds are nearly 2 kpc, the actual distances are probably significantly smaller, since (1) the clouds contribute strongly to the Great Rift obscuration (over most of their projected areas no lower velocity clouds are detected that could produce the obscuration; see Fig. 5); (2) absorption studies indicate a distance of 500 ± 100 pc for the dust in the directions of clouds A and C (Neckel and Klare 1980; FitzGerald 1968), almost no additional absorption being seen between 700 pc and 3 kpc (Forbes 1985); (3) the $R - \Delta V$ relation strongly favors the nearer dust distance (Fig. 10); and (4), although probably due to chance, the alignment of the clouds in longitude with two gaps in the lower velocity lane of emission (Fig. 5) may indicate that, for whatever reason, these clouds have anomalously high LSR velocities.

Cloud A probably contains the dust cloud L673, studied by Herbig and Jones (1983) because it contains the Herbig-Haro object HH 32 and the T Tauri star AS-353 and for which, from an astrometric study of foreground stars, they estimated a rather uncertain distance of 300 pc. We adopt 500 pc as the distance to both clouds A and C, based on the absorption studies and the $R - \Delta V$ relation.

e) Cloud B

The location and velocity of this cloud suggest it may be a small extension of the Aquila Rift. We therefore adopt a distance of 300 pc, equal to the estimated distance of the high-longitude end of the Rift (Sherwood 1974). The cloud coincides closely with a region of roughly uniform obscuration identified by Neckel and Klare (1980); their plot of A_V versus distance for this region contains few stars but is consistent with absorption beginning at 300 pc. The absorption studies of Forbes (1985) and FitzGerald (1968) are also inconclusive but are consistent with our adopted distance, which we estimate to be uncertain by ± 200 pc.

f) Vul OB1

Two very different distances seemed possible for this cloud—the distance of the Vul OB1 association, 2.3 kpc, and the distance of dust in the region estimated from Neckel and Klare (1980), ~ 400 pc. The Vul OB1 association lies toward the center of a partial ring formed by the cloud, and the stellar velocities are comparable to that of the cloud, so an association between the two seemed likely. However, the work of Neckel and Klare (1980) suggested a much smaller distance for dust in this direction. We favor the nearer dust distance because the cloud's narrow line width is not consistent with its being a distant massive cloud (see Fig. 10). In this instance, the $R - \Delta V$ relation was decisive in determining the cloud's distance.

g) Cygnus Rift and Cygnus X

We distinguish the extensive Cygnus Rift from the more intense Cygnus X region which lies behind it. The former is probably part of the system of low-velocity clouds that runs through the first and second quadrants and produces the Great Rift obscuration, while the latter probably results from viewing the Local spiral arm tangentially in a direction of extreme velocity crowding. It is likely that the Cygnus Rift extends in front of the Cygnus X region to $l \approx 86°$, but the Rift cannot be distinguished from Cygnus X because of velocity crowding. Absorption studies along the Cygnus Rift, including regions toward Cygnus X, indicate strong absorption beginning at a distance of $\sim 700 \pm 100$ pc (Neckel and Klare 1980; FitzGerald 1968; Krautter 1980). The velocity and line width of the Cygnus Rift were measured between $l = 64°$ and 74°, where the Rift can be distinguished from Cygnus X. Its area was taken to cover the entire region of the Rift and Cygnus X, and the mass measured between $l = 64°$ and 74° was increased by a factor of 2.9, assuming that the average CO intensity of the Rift above $l = 74°$ is the same as that measured below 74° ($\langle W_{CO} \rangle = 7.1$ K km s^{-1}). The Cygnus X observational parameters were measured in the region of intense emission, $l = 74°$–85°, $b = \pm 2°$. Cong (1977) showed that the Cygnus X region contains numerous large molecular clouds at distances ranging from 500 to 2700 pc; here we adopt the mass-weighted mean distance of the 16 largest clouds identified by Cong, 1700 pc.

h) Cyg OB7

The Cyg OB7 and Cep OB2 associations lie toward the low- and high-longitude edges of this cloud. Since the radial velocities of these associations are comparable to that of the cloud, and since we have found some evidence for interaction with member stars of Cyg OB7 (not presented here), we adopt the distance of both these associations, 800 pc (Humphreys 1978).

REFERENCES

Bedke, J. 1985, private communication.
Bloemen, J. B. G. M., Caraveo, P. A., Hermsen, W., Lebrun, F., Maddalena, R. J., Strong, A. W., and Thaddeus, P. 1984, *Astr. Ap.*, **139**, 37.
Bloemen, J. B. G. M., *et al.* 1985, *Astr. Ap.*, submitted.
Bohlin, R. C., Savage, B. D., and Drake, J. F. 1978, *Ap. J.*, **224**, 132.
Burton, W. B. 1971, *Astr. Ap.*, **10**, 76.
———. 1976, *Ann. Rev. Astr. Ap.*, **14**, 275.
Cesarsky, C. J., Cassé, M., and Paul, J. A. 1977, *Astr. Ap.*, **60**, 139.
Cohen, R. S., Cong, H., Dame, T. M., and Thaddeus, P. 1980, *Ap. J. (Letters)*, **239**, L53.
Cohen, R. S., Dame, T. M., and Thaddeus, P. 1985, *Ap. J. Suppl.*, submitted.
Cong, H. 1977, Ph.D. thesis, Columbia University.
Crampton, D., Georgelin, Y. M., and Georgelin, Y. P. 1978, *Astr. Ap.*, **66**, 1.
Crutcher, R. M., and Lien, D. J. 1985, in *IAU Colloquium 81, Local Interstellar Medium*, ed. Y. Kondo, F. C. Bruhweiler, and B. D. Savage, (NASA Conf. Pub. No. 2345), p. 117.
Dame, T. M. 1984, NASA Tech. Rept., No. 2288.
Dame, T. M., Elmegreen, B. G., Cohen, R. S., and Thaddeus, P. 1985, *Ap. J.*, submitted.
Feitzinger, J. V., and Stuewe, J. A. 1985, in *IAU Colloquium 81, Local Interstellar Medium*, ed. Y. Kondo, F. C. Bruhweiler, and B. D. Savage (NASA Conf. Pub. No. 2345), p. 239.
Fichtel, C. E., Hartman, R. C., Kniffen, D. A., Thompson, D. J., Bignami, G. F., Ögelman, H., Özel, M. E., and Tümer, T. 1975, *Ap. J.*, **198**, 163.
FitzGerald, M. P. 1968, *A.J.*, **73**, 983.
Forbes, D. 1985, *A.J.*, **90**, 301.
Garmany, C. D., Conti, P. S., and Chiosi, C. 1982, *Ap. J.*, **263**, 777.
Gordon, M. A., and Burton, W. B. 1976, *Ap. J.*, **208**, 346.
Heeschen, D. S. 1955, *Ap. J.*, **121**, 569.
Herbig, G. H., and Jones, B. F. 1983, *A.J.*, **88**, 1040.
Huang, Y.-L., Dame, T. M., and Thaddeus, P. 1983, *Ap. J.*, **272**, 609.
Humphreys, R. M. 1978, *Ap. J. Suppl.*, **38**, 309.
Krautter, J. 1980, *Astr. Ap.*, **89**, 74.
Kutner, M. L. 1978, *Ap. Letters*, **19**, 81.
Kutner, M. L., Tucker, K. D., Chin, G., and Thaddeus, P. 1977, *Ap. J.*, **215**, 521.
Lebrun, F., *et al.* 1983, *Ap. J.*, **274**, 231.
Lebrun, F., and Huang, Y.-L. 1984, *Ap. J.*, **281**, 634.
Lindblad, P. O. 1967, *Bull. Astr. Inst. Netherlands*, **19**, 34.
Lindblad, P. O., Grape, K., Sandqvist, Aa., and Schober, J. 1973, *Astr. Ap.*, **24**, 309.
Linsky, J. L. 1973, *Solar Phys.*, **28**, 409.
Lucke, P. B. 1978, *Astr. Ap.*, **64**, 367.
Lynds, B. T. 1962, *Ap. J. Suppl.*, **7**, 1.
Maddalena, R. J., Morris, M., Moscowitz, J., and Thaddeus, P. 1985, *Ap. J.*, submitted.
Myers, P. C., Ho, P. T. P., Schneps, M. H., Chin, G., Pankonin, V., and Winnberg, A. 1978, *Ap. J.*, **220**, 864.
Neckel, T., and Klare, G. 1980, *Astr. Ap. Suppl.*, **42**, 251.
Penzias, A. A., and Burrus, C. A. 1973, *Ann. Rev. Astr. Ap.*, **11**, 51.
Rampino, M. R., and Stothers, R. B. 1984, *Nature*, **308**, 709.
Riegel, K. W., and Crutcher, R. M. 1972, *Astr. Ap.*, **18**, 55.
Sanders, D. B., Solomon, P. M., and Scoville, N. Z. 1984, *Ap. J.*, **276**, 182.
Scoville, N. Z., and Solomon, P. M. 1975, *Ap. J. (Letters)*, **199**, L105.
Sherwood, W. A. 1974, *Pub. Roy. Obs. Edinburgh*, **9**, 85.
Stecker, F. W., Solomon, P. M., Scoville, N. Z., and Ryter, C. E. 1975, *Ap. J.*, **201**, 90.
Thaddeus, P. 1982, in *Symposium on the Orion Nebula to Honor Henry Draper*, ed. A. E. Glassgold, P. J. Huggins, and E. L. Shucking (*Ann. NY Acad. Sci.*, **395**, 9).
Thaddeus, P., and Chanan, G. A. 1985, *Nature*, **314**, 73.

Note added in proof.—During the observing season just ended (1984–1985) a significant improvement of the present survey was completed in collaboration with I. Grenier. Using a new, very sensitive SIS receiver on the 1.2 m telescope, the entire region covered here was reobserved at an angular resolution of 0°.5 (i.e., a 4 × 4 raster), with improved sensitivity: 0.2 K rms at $\Delta v = 1.3$ km s^{-1}. Further, the survey was extended in latitude to uniformly cover $\pm 10°$. A summary of this survey, with improved versions of the basis survey maps, is being submitted to the *Supplement Series of The Astrophysical Journal.*

T. M. DAME and P. THADDEUS: Goddard Institute for Space Studies, 2880 Broadway, New York, NY 10025